Jyväskylän yliopiston julkaisuarkisto
Jyväskylä University Digital Archive

UNIVERSITY OF JYVÄSKYLÄ

This is an electronic reprint of the original article.
This reprint *may differ* from the original in pagination and typographic detail.

Author(s): ALICE Collaboration

Title: Coherent ψ(2S) photo-production in ultra-peripheral Pb-Pb collisions at √sNN=2.76 TeV

Year: 2015

Version:

Please cite the original version:

ALICE Collaboration. (2015). Coherent ψ(2S) photo-production in ultra-peripheral Pb-Pb collisions at √sNN=2.76 TeV. Physics Letters B, 751, 358-370. https://doi.org/10.1016/j.physletb.2015.10.040

All material supplied via JYX is protected by copyright and other intellectual property rights, and duplication or sale of all or part of any of the repository collections is not permitted, except that material may be duplicated by you for your research use or educational purposes in electronic or print form. You must obtain permission for any other use. Electronic or print copies may not be offered, whether for sale or otherwise to anyone who is not an authorised user.

Physics Letters B 751 (2015) 358–370

Contents lists available at ScienceDirect

Physics Letters B

www.elsevier.com/locate/physletb

Coherent $\psi(2S)$ photo-production in ultra-peripheral Pb–Pb collisions at $\sqrt{s_{NN}} = 2.76$ TeV

ALICE Collaboration *

ARTICLE INFO

Article history:
Received 23 August 2015
Received in revised form 14 October 2015
Accepted 14 October 2015
Available online 23 October 2015
Editor: L. Rolandi

ABSTRACT

We have performed the first measurement of the coherent $\psi(2S)$ photo-production cross section in ultra-peripheral Pb–Pb collisions at the LHC. This charmonium excited state is reconstructed via the $\psi(2S) \to l^+l^-$ and $\psi(2S) \to J/\psi\pi^+\pi^-$ decays, where the J/ψ decays into two leptons. The analysis is based on an event sample corresponding to an integrated luminosity of about 22 μb^{-1}. The cross section for coherent $\psi(2S)$ production in the rapidity interval $-0.9 < y < 0.9$ is $d\sigma^{coh}_{\psi(2S)}/dy = 0.83 \pm 0.19(\text{stat} + \text{syst})$ mb. The $\psi(2S)$ to J/ψ coherent cross section ratio is $0.34^{+0.08}_{-0.07}(\text{stat} + \text{syst})$. The obtained results are compared to predictions from theoretical models.

© 2015 CERN for the benefit of the ALICE Collaboration. Published by Elsevier B.V. This is an open access article under the CC BY license (http://creativecommons.org/licenses/by/4.0/). Funded by SCOAP³.

1. Introduction

Two-photon and photo-nuclear interactions at unprecedented energies can be studied in heavy-ion Ultra-Peripheral Collisions (UPC) at the LHC. In such collisions the nuclei are separated by impact parameters larger than the sum of their radii and therefore hadronic interactions are strongly suppressed. The cross sections for photon induced reactions remain large because the strong electromagnetic field of the nucleus enhances the intensity of the photon flux, which grows as the square of the charge of the nucleus. The physics of ultra-peripheral collisions is reviewed in [1,2]. Exclusive photo-production of vector mesons at high energy, where a vector meson is produced in an event with no other final state particles, is of particular interest, since it provides a measure of the nuclear gluon distribution at low Bjorken-x.

Exclusive production of charmonium in photon–proton interactions at HERA [3–5], $\gamma + p \to J/\psi(\psi(2S)) + p$, has been successfully modelled in terms of the exchange of two gluons with no net-colour transfer [6]. Experimental data on this process from HERA have been used to constrain the proton gluon distribution at low Bjorken-x [7]. Exclusive vector meson production in heavy-ion interactions is expected to probe the nuclear gluon distribution [8], for which there is considerable uncertainty in the low-x region [9]. Exclusive ρ^0 [10] and J/ψ [11] production has been studied in Au–Au collisions at RHIC. The exclusive photo-production can be either coherent, where the photon couples coherently to almost all the nucleons, or incoherent, where the photon couples to a single nucleon. Coherent production is characterized by low transverse momenta of vector mesons ($p_T \simeq 60$ MeV/c) where the target nucleus normally does not break up. However, the exchange of additional photons, radiated independently from the original one, may lead to the target nucleus breaking up or de-excite through neutron emission. Simulation models estimate this occurs in about 30% of the events [12]. Incoherent production is characterized by a somewhat higher transverse momentum of the vector mesons ($p_T \simeq 500$ MeV/c). In this case the nucleus interacting with the photon breaks up but, apart from single nucleons or nuclear fragments in the very forward region, no other particles are produced besides the vector meson.

We published the first results on the coherent photo-production of J/ψ in UPC Pb–Pb collisions at the LHC [13] in the rapidity region $-3.6 < y < -2.6$, which constrain the nuclear gluon distribution at Bjorken-$x \simeq 10^{-2}$. Shortly afterwards, ALICE published a second paper measuring both the coherent and the incoherent J/ψ vector meson cross section at mid-rapidity [14], allowing the nuclear gluon distribution at Bjorken-$x \simeq 10^{-3}$ to be explored. The present analysis is performed in the same rapidity region with respect to the measurement reported in [14], and it is sensitive to Bjorken-$x \simeq 10^{-3}$ too.

There are very few studies of photo-production of $\psi(2S)$ off nuclei. Incoherent photo-production, using a 21 GeV photon beam off a deuterium target, has been studied in [15]; non-exclusive photo-production, using bremsstrahlung photons with an average energy of 90 GeV off a ^{6}Li target, have been reported in [16]. However, no previous measurements of $\psi(2S)$ coherent photo-production off nuclear targets have been reported in the literature.

* *E-mail address:* alice-publications@cern.ch.

http://dx.doi.org/10.1016/j.physletb.2015.10.040
0370-2693/© 2015 CERN for the benefit of the ALICE Collaboration. Published by Elsevier B.V. This is an open access article under the CC BY license (http://creativecommons.org/licenses/by/4.0/). Funded by SCOAP³.

In this letter, results from ALICE on exclusive coherent photo-production of $\psi(2S)$ mesons at mid-rapidity in ultra-peripheral Pb–Pb collisions at $\sqrt{s_{\mathrm{NN}}} = 2.76$ TeV are presented. The measured coherent $\psi(2S)$ cross section and the $\psi(2S)/\mathrm{J}/\psi$ cross section ratio are compared to model predictions [17–22].

2. Detector description

The main components of the ALICE detector are a central barrel placed in a large solenoid magnet (B = 0.5 T), covering the pseudo-rapidity region $|\eta| < 0.9$, and a muon spectrometer at forward rapidity, covering the range $-4.0 < \eta < -2.5$ [23]. Three central barrel detectors are used in this analysis. The ALICE Internal Tracking System (ITS) is made of six silicon layers, all of them used in this analysis for particle tracking. The Silicon Pixel Detector (SPD) makes up the two innermost layers of the ITS, covering pseudo-rapidity ranges $|\eta| < 2$ and $|\eta| < 1.4$, for the inner (radius 3.9 cm) and outer (average radius 7.6 cm) layers, respectively. The SPD is a fine granularity detector, having about 10^7 pixels, and is used for triggering purposes. The Time Projection Chamber (TPC) is used for tracking and for particle identification [24] and has an acceptance covering the pseudo-rapidity region $|\eta| < 0.9$. The Time-of-Flight detector (TOF) surrounds the TPC and is a large cylindrical barrel of Multigap Resistive Plate Chambers (MRPC) with about 150,000 readout channels, giving very high precision timing. The TOF pseudo-rapidity coverage matches that of the TPC. Used in combination with the tracking system, the TOF detector is used for charged particle identification up to a transverse momentum of about 2.5 GeV/c (pions and kaons) and 4 GeV/c (protons). In addition, the TOF detector is also used for triggering [25].

The analysis presented below also makes use of two forward detectors. The V0 counters consist of two arrays of 32 scintillator tiles each, covering the range $2.8 < \eta < 5.1$ (V0-A, on the opposite side of the muon spectrometer) and $-3.7 < \eta < -1.7$ (V0-C, on the same side as the muon spectrometer) and positioned respectively at $z = 340$ cm and $z = -90$ cm from the interaction point.

Finally, two sets of hadronic Zero Degree Calorimeters (ZDC) are located at 114 m on either side of the interaction point. The ZDCs detect neutrons emitted in the very forward and backward regions ($|\eta| > 8.7$), such as neutrons produced by electromagnetic dissociation of the nucleus [26] (see Section 3).

3. Data analysis

The event sample considered for the present analysis was collected during the 2011 Pb–Pb run, using a dedicated Barrel Ultra-Peripheral Collision trigger (BUPC), selecting events with the following characteristics:

(i) at least two hits in the SPD detector;
(ii) a number of fired pad-OR (N^{on}) in the TOF detector [25] in the range $2 \le N^{on} \le 6$, with at least two of them with a difference in azimuth, $\Delta\phi$, in the range $150° \le \Delta\phi \le 180°$;
(iii) no hits in the V0-A and no hits in the V0-C detectors.

The integrated luminosity used in this analysis was $22.4^{+0.9}_{-1.2}$ μb^{-1}. Luminosity determination and systematics are discussed in Section 3.1. In the present analysis, coherent $\psi(2S)$ photo-production was studied in four different channels: $\psi(2S) \to l^+l^-$ and $\psi(2S) \to \mathrm{J}/\psi\pi^+\pi^-$, followed by the $\mathrm{J}/\psi \to l^+l^-$ decay, where l^+l^- can be either a e^+e^- or $\mu^+\mu^-$ pair.

3.1. The $\psi(2S) \to l^+l^-$ channel

For the di-muon and di-electron decay channels the following selection criteria were applied:

(i) a reconstructed primary vertex. The primary vertex position is determined from the tracks reconstructed in the ITS and TPC as described in Ref. [27]. The vertex reconstruction algorithm is fully efficient for events with at least one reconstructed primary charged particle in the common TPC and ITS acceptance;
(ii) only two good tracks with at least 70 TPC clusters and at least 1 SPD cluster each. Moreover, particles originated in secondary hadronic interactions or conversions in the detector material, were removed using a distance of closest approach (DCA) cut. The tracks extrapolated to the reconstructed vertex should have a DCA in the beam direction $DCA_L \le 2$ cm, and in the plane orthogonal to the beam direction $DCA_T \le 0.0182 + 0.0350/p_{\mathrm{T}}^{1.01}$, where p_{T} is the transverse momentum in (GeV/c) [28];
(iii) at least one of the two good tracks selected in criterion (ii) should have $p_{\mathrm{T}} \ge 1$ GeV/c; this cut reduces the background, while it marginally affects the genuine leptons from J/ψ decays;
(iv) the V0 trigger required no signal within a time window of 25 ns around the collision time in any of the scintillator tiles of both V0-A and V0-C. Signals in both V0 detectors were searched offline in a larger window according to the prescription described in [14];
(v) the specific energy loss $\mathrm{d}E/\mathrm{d}x$ for the two tracks is compatible with that of electrons or muons (see below); it is worth noting that the TPC resolution does not allow muon and charged pion discrimination;
(vi) the two tracks have opposite charges.

The optimization of the selection criteria to tag efficiently the $\psi(2S)$ was tailored by using the STARLIGHT [17] event generator combined with the ALICE detector full simulation. About 950,000 coherent and incoherent events were simulated for each decay channel. The event total transverse momentum reconstruction is obtained adding the p_T of the two leptons. The selection of coherent events requires a threshold on the reconstruction of the event total transverse momentum, obtained by adding the p_T of the two decay leptons. Transverse momentum carried away by the bremsstrahlung photons reflects in a broadening of the event total p_T. Bremsstrahlung effects are more important for the di-electron decay and the corresponding p_T threshold has to be larger in this case. Consequently a p_T cut $p_T < 0.15$ GeV/c for di-muons and $p_T < 0.3$ GeV/c for di-electrons: 98 (77)% of the coherent signal is retained for di-muons and di-electrons respectively. Fig. 1 (top panel) shows the invariant mass (left) and the p_T distribution (right) for these decay channels. The p_T distributions clearly show a coherent peak at low p_T. No events are found with a transverse momentum exceeding 1.5 GeV/c, as expected for a negligible hadronic contamination, characterized by a much larger event p_T. The number of $\psi(2S)$ candidates are obtained by fitting the invariant mass distribution of both channels to an exponential function describing the underlying continuum and to a Crystal Ball function to extract the $\psi(2S)$ signal. The Crystal Ball $\psi(2S)$ resonance mass and width were left free, while the tail parameters (α and n) were fixed to the values obtained by Monte Carlo simulation. The mass (width calculated from the standard deviation) value from the fit is 3.664 ± 0.013 GeV/c^2 (22 ± 9 MeV/c^2) in good agreement with the known value of the $\psi(2S)$ mass and compatible with the absolute calibration accuracy of the barrel. The obtained yield (see Table 1) was $N^{\mathrm{yield}} = (18.4 \pm 9.3)$.

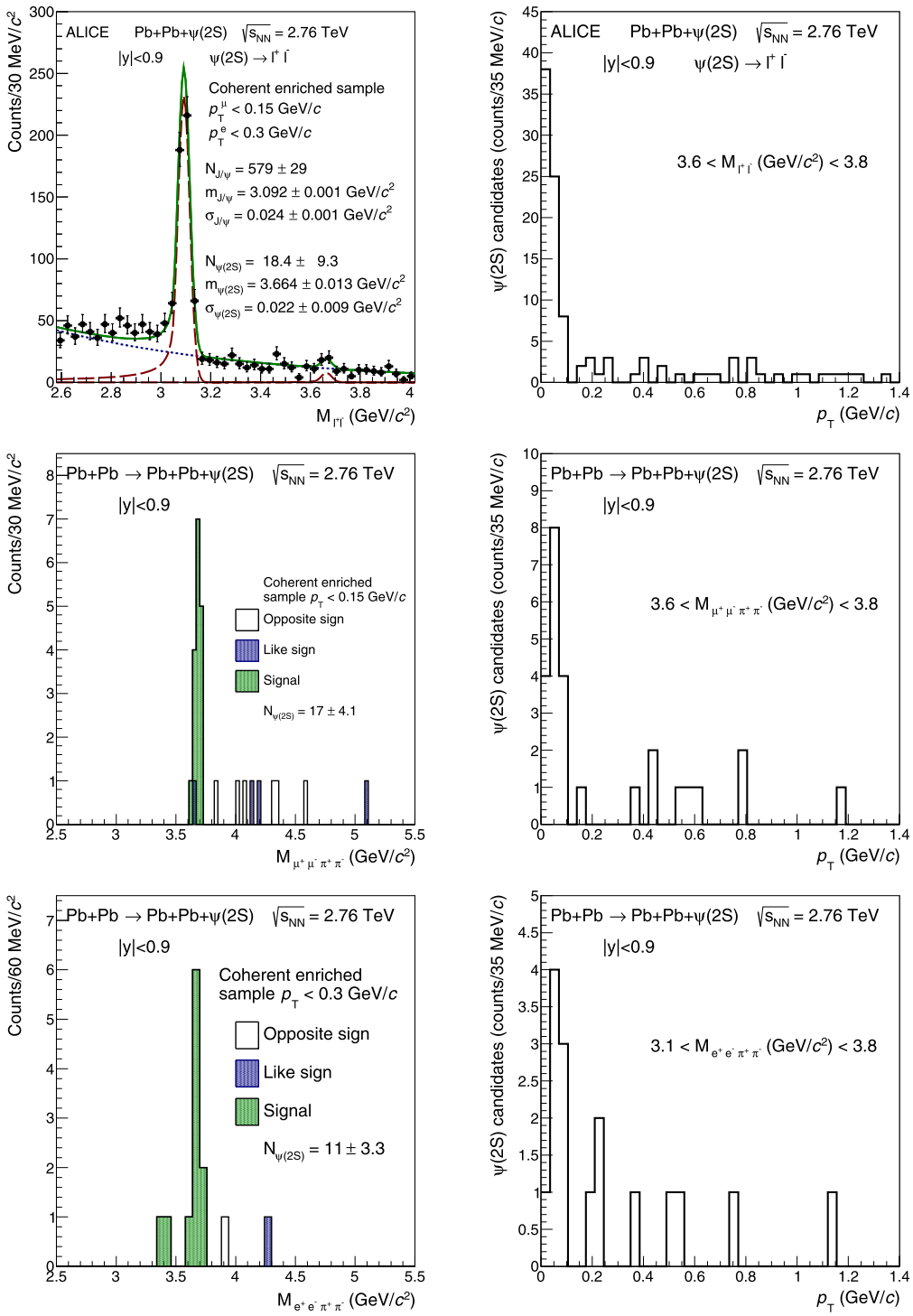

Fig. 1. Invariant mass (left) and p_T distributions (right) for ultra-peripheral Pb–Pb collisions at $\sqrt{s_{NN}} = 2.76$ TeV and $-0.9 < y < 0.9$ for events satisfying the event selections in Section 3. The channels $\psi(2S) \to l^+l^-$ are shown on the top panel ($l^+l^- = e^+e^-$ and $\mu^+\mu^-$), the $\psi(2S) \to \pi^+\pi^-\mu^+\mu^-$ channel is shown in the central and the channel $\psi(2S) \to \pi^+\pi^-e^+e^-$ in the bottom one. The number of event is obtained by the fit (top panel) or by event counting in a selected invariant mass region (central and bottom panel), see text.

The product of the acceptance and efficiency correction $(\mathrm{Acc} \times \varepsilon)_{\psi(2S)}$ was calculated as the ratio of the number of simulated events that satisfy the conditions i) to vi), to the number of generated events with the $\psi(2S)$ in the rapidity interval $-0.9 < y < 0.9$. Transverse polarization of the $\psi(2S)$ is expected from helicity conservation for a quasi-real photon. In addition, for the coherent sample, a reconstructed $\psi(2S)$ transverse momentum condition $p_T < 0.15$ GeV/c ($p_T < 0.3$ GeV/c) was required for di-muons (di-electrons) in the final state. The values for the combined acceptance and efficiency are reported in Table 1.

According to STARLIGHT the fraction (f_I) of incoherent over coherent events in the low p_T region is 4.4% for di-muons and 16.6% for di-electrons. Another theoretical model, described in [22], predicts a much higher coherent over incoherent cross section ratio,

Table 1
Summary of the main experimental results and correction parameters used in the cross section evaluation. The bottom line shows the cross section for the three $\psi(2S)$ decay channels.

	$\psi(2S) \to l^+l^-$	$\psi(2S) \to \mu^+\mu^-\pi^+\pi^-$	$\psi(2S) \to e^+e^-\pi^+\pi^-$
Signal counts	18.4 ± 9.3	17 ± 4.1	11.0 ± 3.3
Bkg. counts (N^{back})	0	1	0
f_I	$(5.6 \pm 1.8)\%$	$(3.4 \pm 1.1)\%$	$(13.2 \pm 4.3)\%$
$(\mathrm{Acc} \times \varepsilon)_{\psi(2S)}$	$(3.65 \pm 0.16)\%$	$(2.35 \pm 0.14)\%$	$(1.33 \pm 0.08)\%$
BR	$(1.56 \pm 0.11)\%$	$(2.02 \pm 0.03)\%$	$(2.02 \pm 0.03)\%$
$\mathscr{L}_{\mathrm{int}}$	$(22.4^{+0.9}_{-1.2})$ μb^{-1}	$(22.4^{+0.9}_{-1.2})$ μb^{-1}	$(22.4^{+0.9}_{-1.2})$ μb^{-1}
Δy	1.8	1.8	1.8
$\frac{d\sigma^{\mathrm{coh}}_{\psi(2S)}}{dy}$ (mb)	$0.76 \pm 0.40(\mathrm{stat}) \pm 0.13(\mathrm{syst})$	$0.81 \pm 0.22(\mathrm{stat})^{+0.09}_{-0.10}(\mathrm{syst})$	$0.90 \pm 0.31(\mathrm{stat})^{+0.13}_{-0.12}(\mathrm{syst})$

resulting in a f_I prediction 50% smaller. Taking the average of these two predictions, $(3.3 \pm 1.1)\%$ for di-muons and $(11.1 \pm 3.4)\%$ for di-electrons is obtained. The uncertainty was obtained by requiring the used value to agree with the two models within 1σ. The final f_I (see Table 1) is the average of the f_I for di-electrons and di-muons, weighted with the corresponding acceptance and efficiency ($\mathrm{Acc} \times \varepsilon$). The remaining background (N_{back}) was estimated studying the wrong-sign event sample, obtained by applying cuts (i) to (v). For di-muon and di-electron channels no wrong-sign events were found in the invariant mass range considered and therefore $N_{back} = 0$.

The coherent $\psi(2S)$ yield is obtained using the formula

$$N^{\mathrm{coh}}_{\psi(2S)} = \frac{N^{\mathrm{yield}} - N^{\mathrm{back}}}{1 + f_I}, \tag{1}$$

giving $N^{\mathrm{coh}}_{\psi(2S)} = 17.5 \pm 9.0$. The coherent $\psi(2S)$ differential cross section can be written as:

$$\frac{d\sigma^{\mathrm{coh}}_{\psi(2S)}}{dy} = \frac{N^{\mathrm{coh}}_{\psi(2S)}}{(\mathrm{Acc} \times \varepsilon)_{\psi(2S)} \cdot \mathscr{L}_{\mathrm{int}} \cdot \Delta y \cdot BR(\psi(2S) \to l^+l^-)}, \tag{2}$$

where $(\mathrm{Acc} \times \varepsilon)_{\psi(2S)}$ corresponds to the acceptance and efficiency as discussed above. $BR(\psi(2S) \to l^+l^-)$ is the branching ratio for $\psi(2S)$ decay into leptons [29], $\Delta y = 1.8$ the rapidity bin size, and $\mathscr{L}_{\mathrm{int}}$ the total integrated luminosity. These values are listed in Table 1. The systematic uncertainty on the yield for the dilepton channel is obtained by varying the bin size and by replacing the exponential with a polynomial to fit the $\gamma\gamma$ process. In addition, the Crystal Ball function parameters can be also obtained by fitting a simulated sample made of $\psi(2S)$ and $\gamma\gamma$ event cocktail and then used to fit the coherent-enriched data sample too. By applying the different methods reported above, the maximum difference in the obtained yield is 12%: this value is used as systematic uncertainty on the yield. The STARLIGHT model predicts a dependence of the $\psi(2S)$ cross section on the rapidity, giving a $\approx 10\%$ variation over the rapidity range $-0.9 < y < 0.9$. In order to evaluate the systematic uncertainty on the acceptance coming from the generator choice, a flat dependence of $d\sigma_{\psi(2S)}/dy$ in the interval $-0.9 < y < 0.9$, as predicted by other models, was used. The relative differences in $(\mathrm{Acc} \times \varepsilon)$ between the input shapes was 1.0%, and are taken into account in the systematic uncertainty calculation. The systematic uncertainty on the tracking efficiency was estimated by comparing, in data and in Monte Carlo, the ITS (TPC) hit matching efficiency to tracks reconstructed with TPC (ITS) hits only.

The trigger efficiency was measured relying on a data sample collected in a dedicated run triggered by the ZDCs only. Events with a topology having the BUPC conditions, given at the beginning of Section 3, were selected. The resulting trigger efficiency was compared to that obtained by the Monte Carlo simulation, showing an agreement within $^{+4.0\%}_{-9.0\%}$.

The e/μ separation was obtained by using two methods:

a) a sharp cut in the scatter plot of the first lepton dE/dx as a function of the second lepton dE/dx, where all the particles beyond a given threshold are considered as electrons;
b) using the average of the electron (muon) dE/dx and considering as electrons (muons) the particles within three sigmas from the Bethe–Block expectation. The difference between the two methods was used as an estimate of the systematic uncertainty, giving ±2%.

The systematic uncertainty related to the application of the V0 offline decision (cut iv) on Section 3.1, was evaluated repeating the analysis with this cut excluded. This results in a more relaxed event selection, increasing the cross section by 6%.

The integrated luminosity was measured using a trigger for the most central hadronic Pb–Pb collisions. The cross section for this process was obtained with a van der Meer scan [30], giving a cross section $\sigma = 4.10^{+0.22}_{-0.13}(\mathrm{syst})$ b [31]. The integrated luminosity for the BUPC trigger sample, corrected for trigger live time, was $\mathscr{L}_{\mathrm{int}} = 22.4^{+0.9}_{-1.2}$ μb^{-1}, where the uncertainty is the quadratic sum of the cross section uncertainty quoted above and the trigger dead time uncertainty. An alternative method based on using neutrons detected in the two ZDCs was also used. The ZDC trigger condition required a signal in at least one of the two calorimeters, thus selecting single electromagnetic dissociation as well as hadronic interactions. The cross section for this trigger was also measured with a van der Meer scan [26]. The integrated luminosity obtained for the BUPC by this method is consistent with the one quoted above within 2.5%. The sources and the values of the systematic uncertainties are listed in Table 2. As a result in the rapidity interval $-0.9 < y < 0.9$ a cross section $d\sigma^{\mathrm{coh}}_{\psi(2S)}/dy = 0.76 \pm 0.40(\mathrm{stat})^{+0.12}_{-0.13}(\mathrm{syst})$ mb is obtained.

3.2. The $\psi(2S) \to \pi^+\pi^- J/\psi$, $J/\psi \to l^+l^-$ ($l^+l^- = e^+e^-, \mu^+\mu^-$) channels

The analysis criteria used to select these channels are similar to those described in Section 3.1, with the requirements on the track quality slightly relaxed to keep the efficiency at an acceptable level. Such a cut softening was allowed by the smaller QED background in four track events, compared to the channels described in Section 3.1. Selection (ii) is modified so that four good tracks with at least 50 TPC clusters each are required. In addition to cuts i) to vi), the invariant mass of di-muons (di-electrons) was required to match that expected by leptons from J/ψ decay, i.e. $3.0 < M_{\pi^+\pi^-\mu^+\mu^-} < 3.2$ GeV/c^2 for di-muons ($2.6 < M_{\pi^+\pi^-e^+e^-} < 3.2$ GeV/c^2 for di-electrons).

The acceptance and the efficiency were estimated with similar techniques. Due to the coupling to the photon, the $\psi(2S)$ is transversely polarized. According to previous experiments [32], J/ψ and

Table 2
Systematic uncertainties per decay channel.

		$\psi(2S) \to l^+l^-$	$\psi(2S) \to \mu^+\mu^-\pi^+\pi^-$	$\psi(2S) \to e^+e^-\pi^+\pi^-$
Signal extraction		±12%	< 1%	< 1%
Incoherent contamination (f_I)		±1.8%	±1.3%	±4.8%
(Acc × ε)	Generator $\frac{d\sigma}{dy}$	±1%	±2%	±2%
	Tracking efficiency	±4.2%	±6.0%	±6.0%
Trigger efficiency		$^{+4\%}_{-9\%}$	$^{+4\%}_{-9\%}$	$^{+4\%}_{-9\%}$
e/μ separation		±2%	±2%	±2%
V0 offline decision		$^{+6\%}_{-0\%}$	$^{+6\%}_{-0\%}$	$^{+9\%}_{-0\%}$
Luminosity		$^{+5.5\%}_{-4.0\%}$	$^{+5.5\%}_{-4.0\%}$	$^{+5.5\%}_{-4.0\%}$
Branching ratio		±7.1%	±1.5%	±1.5%
Uncorrelated sources		±13%	±2%	±5%
Correlated sources		$^{+10\%}_{-11\%}$	$^{+11\%}_{-12\%}$	$^{+13\%}_{-12\%}$
Total		±17%	$^{+11\%}_{-12\%}$	$^{+14\%}_{-13\%}$

two pions from $\psi(2S)$ decay are in s-wave state and thus the $\psi(2S)$ polarization fully transfers to the J/ψ. When computing the efficiency and acceptance the $\psi(2S)$ is therefore assumed transversely polarized. A coherent-enriched sample can be obtained by selecting appropriate regions on invariant mass and p_T, tuned by using a Monte Carlo simulation, as described in Section 3.1. The same p_T cuts used in Section 3 were applied. By selecting invariant mass in the interval $3.6 < M_{\pi^+\pi^-\mu^+\mu^-} < 3.8$ GeV/c^2 ($3.1 < M_{\pi^+\pi^-e^+e^-} < 3.8$ GeV/c^2) for the $\psi(2S) \to \pi^+\pi^-\mu^+\mu^-$ ($\psi(2S) \to \pi^+\pi^-e^+e^-$) channel, 95% (87%) of the signal was retained. The striped area in the invariant mass (left) plots on Fig. 1 (central and bottom panels) shows the $\psi(2S)$ candidates satisfying the p_T cut for the two channels. To extract the coherent $\psi(2S)$ yield, the contribution from incoherent $\psi(2S)$ was subtracted as shown in Eq. (1). The background was estimated by looking at events with all the possible combination of wrong-sign tracks. One event was found in the di-muon sample and no events in the di-electron sample. The fraction of the incoherent sample contaminating the coherent sample was estimated as in Section 3.1, and was found to be 3.4% in the $\psi(2S) \to \pi^+\pi^-\mu^+\mu^-$ channel and 13.2% in the $\psi(2S) \to \pi^+\pi^-e^+e^-$ channel. The systematic uncertainty on the yield was obtained by using an alternative set of cuts. According to the kinematics of the $\psi(2S) \to \pi^+\pi^-$J/ψ decay channel, pions are characterized by a small transverse momentum ($p_T < 0.4$ GeV/c), while the lepton transverse momentum exceeds 1.1 GeV/c. Instead of selecting events where the di-lepton invariant mass is close to that of the J/ψ, events were selected according to the kinematics of the decay products of the $\psi(2S)$. All the other cuts were kept as described in Section 3.1. Two alternative selections were considered: (i) a sample where both leptons have a transverse momentum larger than 1.1 GeV/c; and (ii) a sample without any decay product with transverse momentum in the range $0.4 < p_T < 1.2$ GeV/c. The $\psi(2S)$ yield was unchanged for both these selections while a small change applies to the acceptance and efficiency in the $\pi^+\pi^-$J/ψ decay, giving a negligible systematic uncertainty. The relative difference in (Acc × ε) between the STARLIGHT rapidity shape and a flat rapidity one was 2.0% for $\psi(2S) \to \pi^+\pi^-$J/ψ channel, and is taken into account in the systematic uncertainty calculation. As a result the obtained cross sections in the rapidity interval $-0.9 < y < 0.9$ are $d\sigma^{coh}_{\psi(2S)}/dy = 0.81 \pm 0.22(\text{stat})^{+0.09}_{-0.10}(\text{syst})$ mb for the $\psi(2S) \to \pi^+\pi^-$J/ψ, J/$\psi \to \mu^+\mu^-$ channel and $d\sigma^{coh}_{\psi(2S)}/dy = 0.89 \pm 0.31(\text{stat})^{+0.13}_{-0.12}(\text{syst})$ mb for the $\psi(2S) \to \pi^+\pi^-$J/ψ, J/$\psi \to e^+e^-$ channel.

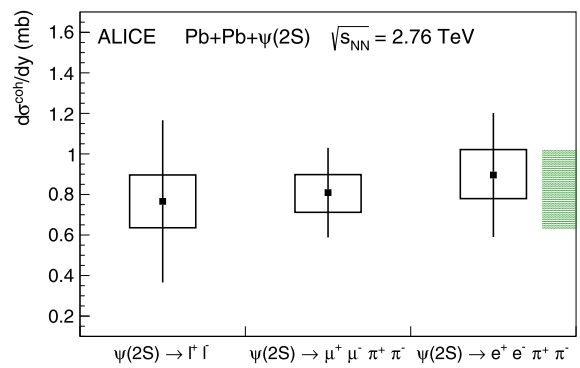

Fig. 2. Measured differential cross section of $\psi(2S)$ photo-production in Pb–Pb ultra-peripheral collisions at $\sqrt{s_{NN}} = 2.76$ TeV at $-0.9 < y < 0.9$ in three different channels. The square represents the systematic uncertainties while the bar represents the statistic uncertainty. The combined cross section uncertainty (shaded area) was obtained using the prescription from reference [33].

3.3. Combining the cross sections

The $\psi(2S)$ coherent production cross sections reported in the Sections 3.1 and 3.2 (Fig. 2) were combined, using the statistical and the uncorrelated systematic uncertainty as a weight. Finally the correlated systematic uncertainty was added. Asymmetric uncertaintys were combined according to the prescriptions given in [33]. The average cross section in the rapidity interval $-0.9 < y < 0.9$ is $d\sigma^{coh}_{\psi(2S)}/dy = 0.83 \pm 0.19(\text{stat} + \text{syst})$ mb.

3.4. Coherent production with nuclear break up or nucleus de-excitation followed by neutron emission

In UPC one or both nuclei may get excited due to the exchange of additional photons. This excitation may lead to break up of the nucleus via emission of one or more neutrons. The neutron emission was measured by using the ZDC detector, for the events studied in the decay channel, $\psi(2S) \to l^+l^-\pi^+\pi^-$. We found 20 events (71^{+9}_{-11})% with no neutrons on either side (0n, 0n), 8 events (29^{+11}_{-9})% with at least one neutron on either side (Xn), 7 events (25^{+10}_{-8})% with no neutron on one side and at least one neutron on the other one (0n Xn) and 1 event (4^{+8}_{-3})% with at least one neutron on both sides (Xn Xn). Uncertainties on the fraction are obtained assuming a binomial distribution. These fractions are in agreement with predictions by STARLIGHT [12] and RSZ [8], as shown in Table 3.

Table 3
Number of events for different neutron emissions in the $\psi(2S) \to l^+l^-\pi^+\pi^-$ process.

	Data	Fraction	STARLIGHT	RSZ
0n 0n	20	(71^{+9}_{-11})%	66%	70%
Xn	8	(29^{+11}_{-9})%	34%	30%
0n Xn	7	(25^{+11}_{-9})%	25%	23%
Xn Xn	1	(4^{+8}_{-3})%	9%	7%

3.5. The $\psi(2S)$ to J/ψ cross section ratio

In order to compare the coherent $\psi(2S)$ cross section to the previously measured J/ψ cross section [14], we report on the $\psi(2S)/J/\psi$ cross section ratio. Many of the systematic uncertainties of these measurements are correlated and cancel out in the ratio. Since the analysis relies on the same data sample and on the same trigger, the systematic uncertainties for the luminosity evaluation, trigger efficiency, and dead time were considered as fully correlated. Several uncertainties, corresponding to the same quantity, measured at slightly different energies (corresponding to the different masses), are partially correlated, while the uncorrelated part is small. Namely, the systematic uncertainties for e/μ separation and the measurement of the neutron number are strongly correlated and hence can be neglected in the ratio. The systematic uncertainties connected to the signal extraction and the branching ratio are considered uncorrelated between the two measurements. The quadratic sum of these sources together with the statistic uncertainty was used to combine different channels in both measurements. For the combination of asymmetric uncertainties the prescription from reference [33] was used. The value of the ratio is $(d\sigma^{coh}_{\psi(2S)}/dy)/(d\sigma^{coh}_{J/\psi}/dy) = 0.34^{+0.08}_{-0.07}(\text{stat} + \text{syst})$.

4. Discussion

We have previously measured the coherent photo-production cross section for the J/ψ vector meson at mid and forward rapidities [13,14]. The results showed that the measured cross section was in good agreement with models that include a nuclear gluon shadowing consistent with the EPS09 parametrization [9]. Models based on the colour dipole model or hadronic interactions of the J/ψ with nuclear matter were disfavoured. The $\psi(2S)$ is similar to the J/ψ in its composition ($c\bar{c}$) and mass, but it has a more complicated wave function as a consequence of it being a 2S rather than a 1S state, and has a larger radius. There is a consensus view about the presence of a node in the $\psi(2S)$ wavefunction: few authors pointed out that this node gives a natural explanation of the $\psi(2S)$ smaller cross section compared to the J/ψ one; in addition it was argued that the node may give strong cancellations in the scattering amplitude in γ-nucleus interactions [34,35].

In Pb–Pb collisions the poor knowledge of the $\psi(2S)$ wave function as a function of the transverse quark pair separation d makes it difficult to estimate the nuclear matter effects.

There are predictions by five different groups for coherent $\psi(2S)$ production in ultra-peripheral Pb–Pb collisions; some of them published several different calculations (see Fig. 3). The model by Adeluyi and Nguyen (AN) is based on a calculation where the $\psi(2S)$ cross section is directly proportional to the gluon distribution squared [18]. It is essentially the same model used by Adeluyi and Bertulani [36] to calculate the coherent J/ψ cross section, which was found to be in good agreement with the ALICE data, when coupled to the EPS09 shadowing parametrization. The calculations are done for four different parameterizations of the nuclear gluon distribution: EPS08 [37], EPS09 [9], HKN07 [38], and

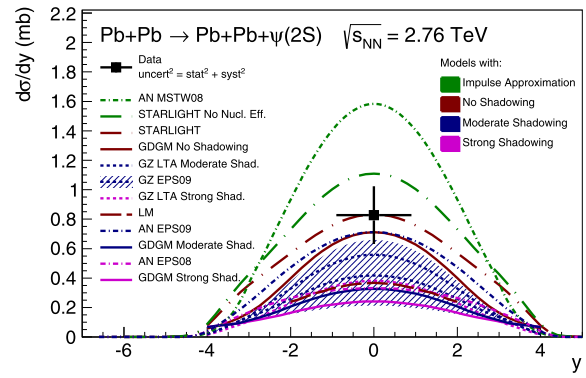

Fig. 3. Measured differential cross section of $\psi(2S)$ photo-production in ultra-peripheral Pb–Pb collisions at $\sqrt{s_{NN}} = 2.76$ TeV at $-0.9 < y < 0.9$. The uncertainty was obtained using the prescription from reference [33]. The theoretical calculations described in the text are also shown.

MSTW08 [39]. The last one (MSTW08) corresponds to a scaling of the γp cross section neglecting any nuclear effects (impulse approximation). It is worth noting they used for the $\psi(2S)$ the same wave function used for the J/ψ. The model by Gay Ducati, Griep, and Machado (GDGM) [19] is based on the colour dipole model and is similar to the model by Goncalves and Machado for coherent J/ψ production [20]. The latter calculation could not reproduce the ALICE coherent J/ψ measurement. The new calculation has, however, been tuned to correctly reproduce the ALICE J/ψ result. The model by Lappi and Mantysaari (LM) is based on the colour dipole model [21]. Their prediction for the J/ψ was about a factor of two above the cross section measured by ALICE. The current $\psi(2S)$ cross section has been scaled down to compensate for this discrepancy. The model by Guzey and Zhalov (GZ) is based on the leading approximation of perturbative QCD [22]. They used different gluon shadowing predictions, using the dynamical leading twist theory or the EPS09 fit. Finally, STARLIGHT uses the Vector Meson Dominance model and a parametrization of the existing HERA data to calculate the $\psi(2S)$ cross section from a Glauber model assuming only hadronic interactions of the $\psi(2S)$ [17]. This model does not implement nuclear gluon shadowing.

It is worth noting that removing all nuclear effects in STARLIGHT gives a cross section for J/ψ production almost identical to the Adeluyi–Bertulani model, if the MSTW08 parametrization is used. The last one corresponds to a scaling of the γ–p cross section neglecting any nuclear effects, i.e. considering all nucleons contributing to the scattering (impulse approximation). Conversely, when applying the same procedure to the $\psi(2S)$ vector meson production, the comparison shows that STARLIGHT cross section is $\simeq 50\%$ smaller with respect to the Adeluyi–Nguyen one. This result may indicate that the $\gamma + \text{p} \to \psi(2S) + \text{p}$ cross section is parametrized in a different way in the two models, due to the limited experimental data, making it difficult to tune the models. For J/ψ, a wealth of $\gamma + p \to J/\psi + p$ cross section data has been obtained by ZEUS and H1, while the process $\gamma + p \to \psi(2S) + p$ was measured by H1 at four different energies only. This makes it much harder to constrain the theoretical cross section to the experimental data. Since the effect of gluon shadowing decreases the vector meson production cross section, this may explain why the $\psi(2S)$ STARLIGHT cross section is close to the AN-EPS09 model, while it is a factor of two larger for J/ψ.

The coherent $\psi(2S)$ photo-production cross section is compared to calculations from twelve different models in Fig. 3. Since a comprehensive model uncertainty is not provided by the model authors, the comparison with the experimental results is quantified by dividing the difference between the value of each model at $y = 0$ and the experimental result, by the uncertainty of the mea-

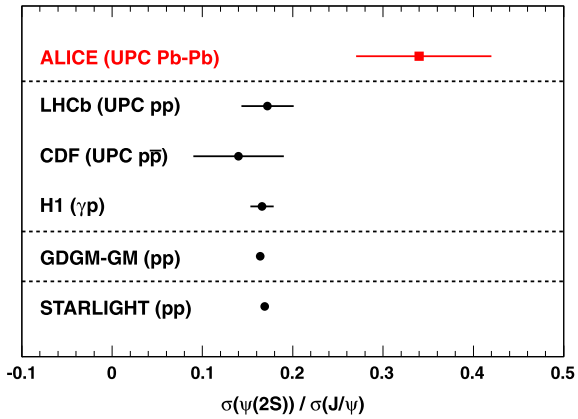

Fig. 4. Ratio of the $\psi(2S)$ to J/ψ cross section for pp and γp interactions compared to theoretical predictions. The ALICE ratio measured in Pb–Pb collisions is shown as well. The uncertainty was obtained using the prescription from reference [33].

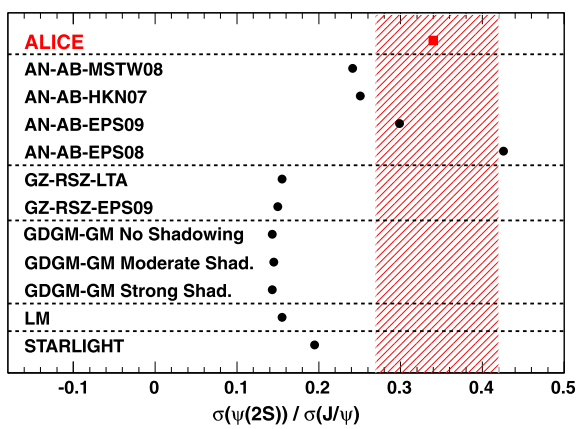

Fig. 5. Ratio of the $\psi(2S)$ to J/ψ cross section measured by ALICE in Pb–Pb collisions. The uncertainty was obtained using the prescription from reference [33]. The predictions from different theoretical models are also shown.

surement itself. The present measurement disfavours the EPS08 parametrization when implemented in the AN model and the GDGM models with a strong shadowing. Similarly the models that neglect any nuclear effect are disfavoured at a level between 1.5 and 3 sigmas. The systematic uncertainties on the cross section parametrization and the experimental statistical uncertainties do not allow a preference to be given between the models implementing moderate nuclear gluon shadowing (as AN-EPS09) and those taking into account Glauber nuclear effects only (as STARLIGHT).

Fig. 4 shows the $\psi(2S)$ to J/ψ cross section ratio measured in Pb–Pb collisions by ALICE and those obtained in p$\bar{\text{p}}$ collisions by CDF [40], and in pp collisions by LHCb [41]. Both STARLIGHT and the GDGM model predict correctly the experimental pp results. The figure also shows the ratio measured by H1 in γp collisions. The H1 result is compatible with the pp measurements, while the ALICE point is 2σ larger than the average of the pp measurements, although still with sizable uncertainties. This difference may indicate that the nuclear effects and/or the gluon shadowing modify the J/ψ and the $\psi(2S)$ production in a different way, since other effects, as the different photon flux, due to the larger $\psi(2S)$ mass, could not explain such a difference.

Fig. 5 shows the comparison of the $\psi(2S)$ to J/ψ cross section ratio between measurements and predictions in Pb–Pb UPC. Most models predict a $\psi(2S)$ to J/ψ cross section ratio in Pb–Pb collisions smaller by 2–2.5 σ than the one measured by ALICE. It is worth noting the same models which reproduced correctly the pp ratio, fail in describing the Pb–Pb ratio. It is surprising that the AN model, although it assumes a $\psi(2S)$ wave function identical to the J/ψ one, describes in a satisfactory way this ratio.

5. Conclusions

We performed the first measurement of the coherent $\psi(2S)$ photo-production cross section in Pb–Pb collisions, obtaining $d\sigma^{coh}_{\psi(2S)}/dy = 0.83 \pm 0.19(\text{stat} + \text{syst})$ mb in the interval $-0.9 < y < 0.9$. This result disfavours models considering all nucleons contributing to the scattering and those implementing strong shadowing, as EPS08 parametrization. The ratio of the $\psi(2S)$ to J/ψ cross section ratio in the rapidity interval $-0.9 < y < 0.9$ is $0.34^{+0.08}_{-0.07}(\text{stat} + \text{syst})$. Most of the models underpredict this ratio by 2–2.5 σ. The current models of the $\psi(2S)$ production in ultra-peripheral collisions require further efforts; the data shown in the present analysis may help to improve the understanding of this process and to refine the theory behind the exclusive vector meson photo-production.

Acknowledgements

The ALICE Collaboration would like to thank all its engineers and technicians for their invaluable contributions to the construction of the experiment and the CERN accelerator teams for the outstanding performance of the LHC complex. The ALICE Collaboration gratefully acknowledges the resources and support provided by all Grid centres and the Worldwide LHC Computing Grid (WLCG) Collaboration. The ALICE Collaboration acknowledges the following funding agencies for their support in building and running the ALICE detector: State Committee of Science, World Federation of Scientists (WFS) and Swiss Fonds Kidagan, Armenia, Conselho Nacional de Desenvolvimento Científico e Tecnológico (CNPq), Financiadora de Estudos e Projetos (FINEP), Fundação de Amparo à Pesquisa do Estado de São Paulo (FAPESP); National Natural Science Foundation of China (NSFC), the Chinese Ministry of Education (CMOE) and the Ministry of Science and Technology of the People's Republic of China (MSTC); Ministry of Education and Youth of the Czech Republic; Danish Natural Science Research Council, the Carlsberg Foundation and the Danish National Research Foundation; The European Research Council under the European Community's Seventh Framework Programme; Helsinki Institute of Physics and the Academy of Finland; French CNRS-IN2P3, the 'Region Pays de Loire', 'Region Alsace', 'Region Auvergne' and CEA, France; German Bundesministerium fur Bildung, Wissenschaft, Forschung und Technologie (BMBF) and the Helmholtz Association; General Secretariat for Research and Technology, Ministry of Development, Greece; Hungarian Orszagos Tudomanyos Kutatasi Alappgrammok (OTKA) and National Office for Research and Technology (NKTH); Department of Atomic Energy and Department of Science and Technology of the Government of India; Istituto Nazionale di Fisica Nucleare (INFN) and Centro Fermi – Museo Storico della Fisica e Centro Studi e Ricerche "Enrico Fermi", Italy; MEXT Grant-in-Aid for Specially Promoted Research, Japan; Joint Institute for Nuclear Research, Dubna; National Research Foundation of Korea (NRF); Consejo Nacional de Ciencia y Tecnología (CONACYT), Direccion General de Asuntos del Personal Academico (DGAPA), México, Amerique Latine Formation academique – European Commission (ALFA-EC) and the EPLANET Program (European Particle Physics Latin American Network); Stichting voor Fundamenteel Onderzoek der Materie (FOM) and the Nederlandse Organisatie voor Wetenschappelijk Onderzoek (NWO), Netherlands; Research Council of Norway (NFR); National Science Centre, Poland; Ministry of

National Education/Institute for Atomic Physics and National Council of Scientific Research in Higher Education (CNCSI-UEFISCDI), Romania; Ministry of Education and Science of the Russian Federation, Russian Academy of Sciences, Russian Federal Agency of Atomic Energy, Russian Federal Agency for Science and Innovations and The Russian Foundation for Basic Research; Ministry of Education of Slovakia; Department of Science and Technology, Republic of South Africa; Centro de Investigaciones Energeticas, Medioambientales y Tecnologicas (CIEMAT), E-Infrastructure shared between Europe and Latin America (EELA), Ministerio de Economía y Competitividad (MINECO) of Spain, Xunta de Galicia (Consellería de Educación), Centro de Aplicaciones Tecnológicas y Desarrollo Nuclear (CEADEN), Cubaenergía, Cuba, and IAEA (International Atomic Energy Agency); Swedish Research Council (VR) and Knut & Alice Wallenberg Foundation (KAW); Ukraine Ministry of Education and Science; United Kingdom Science and Technology Facilities Council (STFC); The United States Department of Energy, the United States National Science Foundation, the State of Texas, and the State of Ohio; Ministry of Science, Education and Sports of Croatia and Unity through Knowledge Fund, Croatia; Council of Scientific and Industrial Research (CSIR), New Delhi, India.

References

[1] A. Baltz, G. Baur, D. d'Enterria, L. Frankfurt, F. Gelis, et al., The physics of ultra-peripheral collisions at the LHC, Phys. Rep. 458 (2008) 1–171, arXiv:0706.3356 [nucl-ex].
[2] C.A. Bertulani, S.R. Klein, J. Nystrand, Physics of ultra-peripheral nuclear collisions, Annu. Rev. Nucl. Part. Sci. 55 (2005) 271–310, arXiv:nucl-ex/0502005.
[3] ZEUS Collaboration, S. Chekanov, et al., Exclusive photoproduction of J/ψ mesons at HERA, Eur. Phys. J. C 24 (2002) 345–360, arXiv:hep-ex/0201043.
[4] H1 Collaboration, C. Alexa, et al., Elastic and proton-dissociative photoproduction of J/ψ mesons at HERA, Eur. Phys. J. C 73 (2013) 2466, arXiv:1304.5162 [hep-ex].
[5] H1 Collaboration, C. Adloff, et al., Diffractive photoproduction of $\psi(2S)$ mesons at HERA, Phys. Lett. B 541 (2002) 251–264, arXiv:hep-ex/0205107.
[6] M. Ryskin, Diffractive J/ψ electroproduction in LLA QCD, Z. Phys. C 57 (1993) 89–92.
[7] A. Martin, C. Nockles, M.G. Ryskin, T. Teubner, Small x gluon from exclusive J/ψ production, Phys. Lett. B 662 (2008) 252–258, arXiv:0709.4406 [hep-ph].
[8] V. Rebyakova, M. Strikman, M. Zhalov, Coherent rho and J/psi photoproduction in ultraperipheral processes with electromagnetic dissociation of heavy ions at RHIC and LHC, Phys. Lett. B 710 (2012) 647–653, arXiv:1109.0737 [hep-ph].
[9] K. Eskola, H. Paukkunen, C. Salgado, EPS09: a new generation of NLO and LO nuclear parton distribution functions, J. High Energy Phys. 0904 (2009) 065, arXiv:0902.4154 [hep-ph].
[10] STAR Collaboration, B. Abelev, et al., rho0 photoproduction in ultraperipheral relativistic heavy ion collisions with STAR, Phys. Rev. C 77 (2008) 034910, arXiv:0712.3320 [nucl-ex].
[11] PHENIX Collaboration, S. Afanasiev, et al., Photoproduction of J/psi and of high mass e + e- in ultra-peripheral Au + Au collisions at $\sqrt{s_{NN}} = 200$-GeV, Phys. Lett. B 679 (2009) 321–329, arXiv:0903.2041 [nucl-ex].
[12] A.J. Baltz, S.R. Klein, J. Nystrand, Coherent vector meson photoproduction with nuclear breakup in relativistic heavy ion collisions, Phys. Rev. Lett. 89 (2002) 012301, arXiv:nucl-th/0205031.
[13] ALICE Collaboration, B. Abelev, et al., Coherent J/ψ photoproduction in ultra-peripheral Pb–Pb collisions at $\sqrt{s_{NN}} = 2.76$ TeV, Phys. Lett. B 718 (2013) 1273–1283, arXiv:1209.3715 [nucl-ex].
[14] ALICE Collaboration, E. Abbas, et al., Charmonium and e^+e^- pair photoproduction at mid-rapidity in ultra-peripheral Pb–Pb collisions at $\sqrt{s_{NN}} = 2.76$ TeV, Eur. Phys. J. C 73 (2013) 2617, arXiv:1305.1467 [nucl-ex].
[15] U. Camerini, J. Learned, R. Prepost, C.M. Spencer, D. Wiser, et al., Photoproduction of the psi particles, Phys. Rev. Lett. 35 (1975) 483.
[16] NA14 Collaboration, R. Barate, et al., Measurement of J/ψ and ψ' real photoproduction on ^{6}Li at a mean energy of 90-GeV, Z. Phys. C 33 (1987) 505.
[17] S. Klein, J. Nystrand, Exclusive vector meson production in relativistic heavy ion collisions, Phys. Rev. C 60 (1999) 014903, arXiv:hep-ph/9902259.
[18] A. Adeluyi, T. Nguyen, Coherent photoproduction of ψ and Υ mesons in ultraperipheral pPb and PbPb collisions at the CERN large hadron collider at $\sqrt{S_{NN}} = 5$ TeV and $\sqrt{S_{NN}} = 2.76$ TeV, Phys. Rev. C 87 (2013) 027901, arXiv:1302.4288 [nucl-th].
[19] M.B.G. Ducati, M. Griep, M. Machado, Diffractive photoproduction of radially excited psi(2S) mesons in photon-Pomeron reactions in PbPb collisions at the CERN LHC, Phys. Rev. C 88 (2013) 014910, arXiv:1305.2407 [hep-ph].
[20] V. Goncalves, M. Machado, Vector meson production in coherent hadronic interactions: an update on predictions for RHIC and LHC, Phys. Rev. C 84 (2011) 011902, arXiv:1106.3036 [hep-ph].
[21] T. Lappi, H. Mantysaari, J/Psi production in ultraperipheral Pb + Pb and p + Pb collisions at LHC energies, Phys. Rev. C 87 (2013) 032201, arXiv:1301.4095 [hep-ph].
[22] V. Guzey, M. Zhalov, Comparison of $\psi(2S)$ and J/ψ photoproduction cross sections in Pb–Pb ultraperipheral collisions at the LHC, arXiv:1404.6101 [hep-ph].
[23] ALICE Collaboration, K. Aamodt, et al., The ALICE experiment at the CERN LHC, J. Instrum. 3 (2008), S08002.
[24] J. Alme, et al., The ALICE TPC, a large 3-dimensional tracking device with fast readout for ultra-high multiplicity events, Nucl. Instrum. Methods A 622 (2010) 316–367, arXiv:1001.1950 [physics.ins-det].
[25] A. Akindinov, et al., A topological trigger based on the Time-of-Flight detector for the ALICE experiment, Nucl. Instrum. Methods A 602 (2009) 372–376.
[26] ALICE Collaboration, B. Abelev, et al., Measurement of the cross section for electromagnetic dissociation with neutron emission in Pb–Pb collisions at $\sqrt{s_{NN}} = 2.76$ TeV, Phys. Rev. Lett. 109 (2012) 252302, arXiv:1203.2436 [nucl-ex].
[27] ALICE Collaboration, B. Abelev, et al., Centrality dependence of charged particle production at large transverse momentum in Pb–Pb collisions at $\sqrt{s_{NN}} = 2.76$ TeV, Phys. Lett. B 720 (2013) 52, arXiv:1208.2711 [hep-ex].
[28] ALICE Collaboration, K. Aamodt, et al., Transverse momentum spectra of charged particles in proton–proton collisions at $\sqrt{s} = 900$ GeV with ALICE at the LHC, Phys. Lett. B 693 (2010) 53, arXiv:1007.0719 [physics.ins-det].
[29] Particle Data Group Collaboration, J. Beringer, et al., Review of particle physics (RPP), Phys. Rev. D 86 (2012) 010001.
[30] S. van der Meer, Calibration of the effective beam height in the ISR, CERN-ISR-PO-68-31, 1968.
[31] ALICE Collaboration, B.B. Abelev, et al., Performance of the ALICE experiment at the CERN LHC, Int. J. Mod. Phys. A 29 (2014) 1430044, arXiv:1402.4476 [nucl-ex].
[32] BES Collaboration, J.Z. Bai, et al., $\psi' \to \pi^+\pi^- J/\psi$ decay distribution, Phys. Rev. D 62 (2000) 032002, arXiv:hep-ex/9909038.
[33] R. Barlow, Asymmetric statistical errors, arXiv:physics/0406120.
[34] J. Nemchik, N.N. Nikolaev, E. Predazzi, B. Zakharov, Color dipole phenomenology of diffractive electroproduction of light vector mesons at HERA, Z. Phys. C 75 (1997) 71–87, arXiv:hep-ph/9605231.
[35] J. Hufner, Y. Ivanov, B. Kopeliovich, A. Tarasov, Photoproduction of charmonia and total charmonium proton cross-sections, Phys. Rev. D 62 (2000) 094022, arXiv:hep-ph/0007111.
[36] A. Adeluyi, C. Bertulani, Constraining gluon shadowing using photoproduction in ultraperipheral pA and AA collisions, Phys. Rev. C 85 (2012) 044904, arXiv:1201.0146 [nucl-th].
[37] K.J. Eskola, H. Paukkunen, C.A. Salgado, An improved global analysis of nuclear parton distribution functions including RHIC data, J. High Energy Phys. 07 (2008) 102, arXiv:0802.0139 [hep-ph].
[38] M. Hirai, S. Kumano, T.-H. Nagai, Determination of nuclear parton distribution functions and their uncertainties in next-to-leading order, Phys. Rev. C 76 (2007) 065207, arXiv:0709.3038 [hep-ph].
[39] A. Martin, W. Stirling, R. Thorne, G. Watt, Parton distributions for the LHC, Eur. Phys. J. C 63 (2009) 189–285, arXiv:0901.0002 [hep-ph].
[40] CDF Collaboration, T. Aaltonen, et al., Observation of exclusive charmonium production and $\gamma + \gamma$ to $\mu^+\mu^-$ in $p\bar{p}$ collisions at $\sqrt{s} = 1.96$ TeV, Phys. Rev. Lett. 102 (2009) 242001, arXiv:0902.1271 [hep-ex].
[41] LHCb Collaboration, R. Aaij, et al., Updated measurements of exclusive J/ψ and $\psi(2S)$ production cross-sections in pp collisions at $\sqrt{s} = 7$ TeV, J. Phys. G 41 (2014) 055002, arXiv:1401.3288 [hep-ex].

ALICE Collaboration

J. Adam [39], D. Adamová [82], M.M. Aggarwal [86], G. Aglieri Rinella [36], M. Agnello [110], N. Agrawal [47], Z. Ahammed [130], S.U. Ahn [67], I. Aimo [93,110], S. Aiola [135], M. Ajaz [16], A. Akindinov [57], S.N. Alam [130], D. Aleksandrov [99], B. Alessandro [110], D. Alexandre [101], R. Alfaro Molina [63], A. Alici [104,12], A. Alkin [3], J. Alme [37], T. Alt [42], S. Altinpinar [18], I. Altsybeev [129], C. Alves Garcia Prado [118], C. Andrei [77], A. Andronic [96],

V. Anguelov [92], J. Anielski [53], T. Antičić [97], F. Antinori [107], P. Antonioli [104], L. Aphecetche [112], H. Appelshäuser [52], S. Arcelli [28], N. Armesto [17], R. Arnaldi [110], T. Aronsson [135], I.C. Arsene [22], M. Arslandok [52], A. Augustinus [36], R. Averbeck [96], M.D. Azmi [19], M. Bach [42], A. Badalà [106], Y.W. Baek [43], S. Bagnasco [110], R. Bailhache [52], R. Bala [89], A. Baldisseri [15], F. Baltasar Dos Santos Pedrosa [36], R.C. Baral [60], A.M. Barbano [110], R. Barbera [29], F. Barile [33], G.G. Barnaföldi [134], L.S. Barnby [101], V. Barret [69], P. Bartalini [7], K. Barth [36], J. Bartke [115], E. Bartsch [52], M. Basile [28], N. Bastid [69], S. Basu [130], B. Bathen [53], G. Batigne [112], A. Batista Camejo [69], B. Batyunya [65], P.C. Batzing [22], I.G. Bearden [79], H. Beck [52], C. Bedda [110], N.K. Behera [47,48], I. Belikov [54], F. Bellini [28], H. Bello Martinez [2], R. Bellwied [120], R. Belmont [133], E. Belmont-Moreno [63], V. Belyaev [75], G. Bencedi [134], S. Beole [27], I. Berceanu [77], A. Bercuci [77], Y. Berdnikov [84], D. Berenyi [134], R.A. Bertens [56], D. Berzano [36,27], L. Betev [36], A. Bhasin [89], I.R. Bhat [89], A.K. Bhati [86], B. Bhattacharjee [44], J. Bhom [126], L. Bianchi [120,27], N. Bianchi [71], C. Bianchin [56,133], J. Bielčík [39], J. Bielčíková [82], A. Bilandzic [79], R. Biswas [4], S. Biswas [78], S. Bjelogrlic [56], F. Blanco [10], D. Blau [99], C. Blume [52], F. Bock [73,92], A. Bogdanov [75], H. Bøggild [79], L. Boldizsár [134], M. Bombara [40], J. Book [52], H. Borel [15], A. Borissov [95], M. Borri [81], F. Bossú [64], M. Botje [80], E. Botta [27], S. Böttger [51], P. Braun-Munzinger [96], M. Bregant [118], T. Breitner [51], T.A. Broker [52], T.A. Browning [94], M. Broz [39], E.J. Brucken [45], E. Bruna [110], G.E. Bruno [33], D. Budnikov [98], H. Buesching [52], S. Bufalino [110,36], P. Buncic [36], O. Busch [92,126], Z. Buthelezi [64], J.T. Buxton [20], D. Caffarri [36], X. Cai [7], H. Caines [135], L. Calero Diaz [71], A. Caliva [56], E. Calvo Villar [102], P. Camerini [26], F. Carena [36], W. Carena [36], J. Castillo Castellanos [15], A.J. Castro [123], E.A.R. Casula [25], C. Cavicchioli [36], C. Ceballos Sanchez [9], J. Cepila [39], P. Cerello [110], B. Chang [121], S. Chapeland [36], M. Chartier [122], J.L. Charvet [15], S. Chattopadhyay [130], S. Chattopadhyay [100], V. Chelnokov [3], M. Cherney [85], C. Cheshkov [128], B. Cheynis [128], V. Chibante Barroso [36], D.D. Chinellato [119], P. Chochula [36], K. Choi [95], M. Chojnacki [79], S. Choudhury [130], P. Christakoglou [80], C.H. Christensen [79], P. Christiansen [34], T. Chujo [126], S.U. Chung [95], Z. Chunhui [56], C. Cicalo [105], L. Cifarelli [12,28], F. Cindolo [104], J. Cleymans [88], F. Colamaria [33], D. Colella [33], A. Collu [25], M. Colocci [28], G. Conesa Balbastre [70], Z. Conesa del Valle [50], M.E. Connors [135], J.G. Contreras [39,11], T.M. Cormier [83], Y. Corrales Morales [27], I. Cortés Maldonado [2], P. Cortese [32], M.R. Cosentino [118], F. Costa [36], P. Crochet [69], R. Cruz Albino [11], E. Cuautle [62], L. Cunqueiro [36], T. Dahms [91], A. Dainese [107], A. Danu [61], D. Das [100], I. Das [100,50], S. Das [4], A. Dash [119], S. Dash [47], S. De [118], A. De Caro [31,12], G. de Cataldo [103], J. de Cuveland [42], A. De Falco [25], D. De Gruttola [12,31], N. De Marco [110], S. De Pasquale [31], A. Deisting [96,92], A. Deloff [76], E. Dénes [134], G. D'Erasmo [33], D. Di Bari [33], A. Di Mauro [36], P. Di Nezza [71], M.A. Diaz Corchero [10], T. Dietel [88], P. Dillenseger [52], R. Divià [36], Ø. Djuvsland [18], A. Dobrin [56,80], T. Dobrowolski [76,i], D. Domenicis Gimenez [118], B. Dönigus [52], O. Dordic [22], A.K. Dubey [130], A. Dubla [56], L. Ducroux [128], P. Dupieux [69], R.J. Ehlers [135], D. Elia [103], H. Engel [51], B. Erazmus [112,36], F. Erhardt [127], D. Eschweiler [42], B. Espagnon [50], M. Estienne [112], S. Esumi [126], J. Eum [95], D. Evans [101], S. Evdokimov [111], G. Eyyubova [39], L. Fabbietti [91], D. Fabris [107], J. Faivre [70], A. Fantoni [71], M. Fasel [73], L. Feldkamp [53], D. Felea [61], A. Feliciello [110], G. Feofilov [129], J. Ferencei [82], A. Fernández Téllez [2], E.G. Ferreiro [17], A. Ferretti [27], A. Festanti [30], J. Figiel [115], M.A.S. Figueredo [122], S. Filchagin [98], D. Finogeev [55], F.M. Fionda [103], E.M. Fiore [33], M.G. Fleck [92], M. Floris [36], S. Foertsch [64], P. Foka [96], S. Fokin [99], E. Fragiacomo [109], A. Francescon [36,30], U. Frankenfeld [96], U. Fuchs [36], C. Furget [70], A. Furs [55], M. Fusco Girard [31], J.J. Gaardhøje [79], M. Gagliardi [27], A.M. Gago [102], M. Gallio [27], D.R. Gangadharan [73], P. Ganoti [87], C. Gao [7], C. Garabatos [96], E. Garcia-Solis [13], C. Gargiulo [36], P. Gasik [91], M. Germain [112], A. Gheata [36], M. Gheata [61,36], P. Ghosh [130], S.K. Ghosh [4], P. Gianotti [71], P. Giubellino [36,110], P. Giubilato [30], E. Gladysz-Dziadus [115], P. Glässel [92], A. Gomez Ramirez [51], P. González-Zamora [10], S. Gorbunov [42], L. Görlich [115], S. Gotovac [114], V. Grabski [63], L.K. Graczykowski [132], A. Grelli [56], A. Grigoras [36], C. Grigoras [36], V. Grigoriev [75], A. Grigoryan [1], S. Grigoryan [65], B. Grinyov [3], N. Grion [109], J.F. Grosse-Oetringhaus [36], J.-Y. Grossiord [128], R. Grosso [36], F. Guber [55], R. Guernane [70], B. Guerzoni [28], K. Gulbrandsen [79], H. Gulkanyan [1], T. Gunji [125], A. Gupta [89], R. Gupta [89], R. Haake [53], Ø. Haaland [18], C. Hadjidakis [50], M. Haiduc [61], H. Hamagaki [125], G. Hamar [134], L.D. Hanratty [101], A. Hansen [79], J.W. Harris [135], H. Hartmann [42], A. Harton [13], D. Hatzifotiadou [104], S. Hayashi [125], S.T. Heckel [52], M. Heide [53], H. Helstrup [37], A. Herghelegiu [77], G. Herrera Corral [11], B.A. Hess [35], K.F. Hetland [37], T.E. Hilden [45], H. Hillemanns [36], B. Hippolyte [54], P. Hristov [36], M. Huang [18], T.J. Humanic [20], N. Hussain [44], T. Hussain [19], D. Hutter [42], D.S. Hwang [21], R. Ilkaev [98], I. Ilkiv [76], M. Inaba [126], C. Ionita [36], M. Ippolitov [75,99], M. Irfan [19], M. Ivanov [96], V. Ivanov [84],

V. Izucheev [111], P.M. Jacobs [73], C. Jahnke [118], H.J. Jang [67], M.A. Janik [132], P.H.S.Y. Jayarathna [120], C. Jena [30], S. Jena [120], R.T. Jimenez Bustamante [96], P.G. Jones [101], H. Jung [43], A. Jusko [101], P. Kalinak [58], A. Kalweit [36], J. Kamin [52], J.H. Kang [136], V. Kaplin [75], S. Kar [130], A. Karasu Uysal [68], O. Karavichev [55], T. Karavicheva [55], E. Karpechev [55], U. Kebschull [51], R. Keidel [137], D.L.D. Keijdener [56], M. Keil [36], K.H. Khan [16], M.M. Khan [19], P. Khan [100], S.A. Khan [130], A. Khanzadeev [84], Y. Kharlov [111], B. Kileng [37], B. Kim [136], D.W. Kim [43,67], D.J. Kim [121], H. Kim [136], J.S. Kim [43], M. Kim [43], M. Kim [136], S. Kim [21], T. Kim [136], S. Kirsch [42], I. Kisel [42], S. Kiselev [57], A. Kisiel [132], G. Kiss [134], J.L. Klay [6], C. Klein [52], J. Klein [92], C. Klein-Bösing [53], A. Kluge [36], M.L. Knichel [92], A.G. Knospe [116], T. Kobayashi [126], C. Kobdaj [113], M. Kofarago [36], T. Kollegger [42,96], A. Kolojvari [129], V. Kondratiev [129], N. Kondratyeva [75], E. Kondratyuk [111], A. Konevskikh [55], C. Kouzinopoulos [36], O. Kovalenko [76], V. Kovalenko [129], M. Kowalski [115], S. Kox [70], G. Koyithatta Meethaleveedu [47], J. Kral [121], I. Králik [58], A. Kravčáková [40], M. Krelina [39], M. Kretz [42], M. Krivda [101,58], F. Krizek [82], E. Kryshen [36], M. Krzewicki [96,42], A.M. Kubera [20], V. Kučera [82], T. Kugathasan [36], C. Kuhn [54], P.G. Kuijer [80], I. Kulakov [42], J. Kumar [47], L. Kumar [78,86], P. Kurashvili [76], A. Kurepin [55], A.B. Kurepin [55], A. Kuryakin [98], S. Kushpil [82], M.J. Kweon [49], Y. Kwon [136], S.L. La Pointe [110], P. La Rocca [29], C. Lagana Fernandes [118], I. Lakomov [36,50], R. Langoy [41], C. Lara [51], A. Lardeux [15], A. Lattuca [27], E. Laudi [36], R. Lea [26], L. Leardini [92], G.R. Lee [101], S. Lee [136], I. Legrand [36], R.C. Lemmon [81], V. Lenti [103], E. Leogrande [56], I. León Monzón [117], M. Leoncino [27], P. Lévai [134], S. Li [7,69], X. Li [14], J. Lien [41], R. Lietava [101], S. Lindal [22], V. Lindenstruth [42], C. Lippmann [96], M.A. Lisa [20], H.M. Ljunggren [34], D.F. Lodato [56], P.I. Loenne [18], V.R. Loggins [133], V. Loginov [75], C. Loizides [73], X. Lopez [69], E. López Torres [9], A. Lowe [134], P. Luettig [52], M. Lunardon [30], G. Luparello [26], P.H.F.N.D. Luz [118], A. Maevskaya [55], M. Mager [36], S. Mahajan [89], S.M. Mahmood [22], A. Maire [54], R.D. Majka [135], M. Malaev [84], I. Maldonado Cervantes [62], L. Malinina [65], D. Mal'Kevich [57], P. Malzacher [96], A. Mamonov [98], L. Manceau [110], V. Manko [99], F. Manso [69], V. Manzari [103,36], M. Marchisone [27], J. Mareš [59], G.V. Margagliotti [26], A. Margotti [104], J. Margutti [56], A. Marín [96], C. Markert [116], M. Marquard [52], N.A. Martin [96], J. Martin Blanco [112], P. Martinengo [36], M.I. Martínez [2], G. Martínez García [112], M. Martinez Pedreira [36], Y. Martynov [3], A. Mas [118], S. Masciocchi [96], M. Masera [27], A. Masoni [105], L. Massacrier [112], A. Mastroserio [33], H. Masui [126], A. Matyja [115], C. Mayer [115], J. Mazer [123], M.A. Mazzoni [108], D. Mcdonald [120], F. Meddi [24], A. Menchaca-Rocha [63], E. Meninno [31], J. Mercado Pérez [92], M. Meres [38], Y. Miake [126], M.M. Mieskolainen [45], K. Mikhaylov [57,65], L. Milano [36], J. Milosevic [22,131], L.M. Minervini [103,23], A. Mischke [56], A.N. Mishra [48], D. Miśkowiec [96], J. Mitra [130], C.M. Mitu [61], N. Mohammadi [56], B. Mohanty [130,78], L. Molnar [54], L. Montaño Zetina [11], E. Montes [10], M. Morando [30], D.A. Moreira De Godoy [112], S. Moretto [30], A. Morreale [112], A. Morsch [36], V. Muccifora [71], E. Mudnic [114], D. Mühlheim [53], S. Muhuri [130], M. Mukherjee [130], H. Müller [36], J.D. Mulligan [135], M.G. Munhoz [118], S. Murray [64], L. Musa [36], J. Musinsky [58], B.K. Nandi [47], R. Nania [104], E. Nappi [103], M.U. Naru [16], C. Nattrass [123], K. Nayak [78], T.K. Nayak [130], S. Nazarenko [98], A. Nedosekin [57], L. Nellen [62], F. Ng [120], M. Nicassio [96], M. Niculescu [61,36], J. Niedziela [36], B.S. Nielsen [79], S. Nikolaev [99], S. Nikulin [99], V. Nikulin [84], F. Noferini [104,12], P. Nomokonov [65], G. Nooren [56], J. Norman [122], A. Nyanin [99], J. Nystrand [18], H. Oeschler [92], S. Oh [135], S.K. Oh [66], A. Ohlson [36], A. Okatan [68], T. Okubo [46], L. Olah [134], J. Oleniacz [132], A.C. Oliveira Da Silva [118], M.H. Oliver [135], J. Onderwaater [96], C. Oppedisano [110], A. Ortiz Velasquez [62], A. Oskarsson [34], J. Otwinowski [96,115], K. Oyama [92], M. Ozdemir [52], Y. Pachmayer [92], P. Pagano [31], G. Paić [62], C. Pajares [17], S.K. Pal [130], J. Pan [133], A.K. Pandey [47], D. Pant [47], V. Papikyan [1], G.S. Pappalardo [106], P. Pareek [48], W.J. Park [96], S. Parmar [86], A. Passfeld [53], V. Paticchio [103], R.N. Patra [130], B. Paul [100], T. Peitzmann [56], H. Pereira Da Costa [15], E. Pereira De Oliveira Filho [118], D. Peresunko [75,99], C.E. Pérez Lara [80], V. Peskov [52], Y. Pestov [5], V. Petráček [39], V. Petrov [111], M. Petrovici [77], C. Petta [29], S. Piano [109], M. Pikna [38], P. Pillot [112], O. Pinazza [104,36], L. Pinsky [120], D.B. Piyarathna [120], M. Płoskoń [73], M. Planinic [127], J. Pluta [132], S. Pochybova [134], P.L.M. Podesta-Lerma [117], M.G. Poghosyan [85], B. Polichtchouk [111], N. Poljak [127], W. Poonsawat [113], A. Pop [77], S. Porteboeuf-Houssais [69], J. Porter [73], J. Pospisil [82], S.K. Prasad [4], R. Preghenella [36,104], F. Prino [110], C.A. Pruneau [133], I. Pshenichnov [55], M. Puccio [110], G. Puddu [25], P. Pujahari [133], V. Punin [98], J. Putschke [133], H. Qvigstad [22], A. Rachevski [109], S. Raha [4], S. Rajput [89], J. Rak [121], A. Rakotozafindrabe [15], L. Ramello [32], R. Raniwala [90], S. Raniwala [90], S.S. Räsänen [45], B.T. Rascanu [52], D. Rathee [86], K.F. Read [123], J.S. Real [70], K. Redlich [76], R.J. Reed [133], A. Rehman [18], P. Reichelt [52], F. Reidt [92,36], X. Ren [7], R. Renfordt [52], A.R. Reolon [71], A. Reshetin [55],

F. Rettig [42], J.-P. Revol [12], K. Reygers [92], V. Riabov [84], R.A. Ricci [72], T. Richert [34], M. Richter [22], P. Riedler [36], W. Riegler [36], F. Riggi [29], C. Ristea [61], A. Rivetti [110], E. Rocco [56], M. Rodríguez Cahuantzi [2], A. Rodriguez Manso [80], K. Røed [22], E. Rogochaya [65], D. Rohr [42], D. Röhrich [18], R. Romita [122], F. Ronchetti [71], L. Ronflette [112], P. Rosnet [69], A. Rossi [36], F. Roukoutakis [87], A. Roy [48], C. Roy [54], P. Roy [100], A.J. Rubio Montero [10], R. Rui [26], R. Russo [27], E. Ryabinkin [99], Y. Ryabov [84], A. Rybicki [115], S. Sadovsky [111], K. Šafařík [36], B. Sahlmuller [52], P. Sahoo [48], R. Sahoo [48], S. Sahoo [60], P.K. Sahu [60], J. Saini [130], S. Sakai [71], M.A. Saleh [133], C.A. Salgado [17], J. Salzwedel [20], S. Sambyal [89], V. Samsonov [84], X. Sanchez Castro [54], L. Šándor [58], A. Sandoval [63], M. Sano [126], G. Santagati [29], D. Sarkar [130], E. Scapparone [104], F. Scarlassara [30], R.P. Scharenberg [94], C. Schiaua [77], R. Schicker [92], C. Schmidt [96], H.R. Schmidt [35], S. Schuchmann [52], J. Schukraft [36], M. Schulc [39], T. Schuster [135], Y. Schutz [112,36], K. Schwarz [96], K. Schweda [96], G. Scioli [28], E. Scomparin [110], R. Scott [123], K.S. Seeder [118], J.E. Seger [85], Y. Sekiguchi [125], I. Selyuzhenkov [96], K. Senosi [64], J. Seo [95,66], E. Serradilla [63,10], A. Sevcenco [61], A. Shabanov [55], A. Shabetai [112], O. Shadura [3], R. Shahoyan [36], A. Shangaraev [111], A. Sharma [89], N. Sharma [60,123], K. Shigaki [46], K. Shtejer [27,9], Y. Sibiriak [99], S. Siddhanta [105], K.M. Sielewicz [36], T. Siemiarczuk [76], D. Silvermyr [83,34], C. Silvestre [70], G. Simatovic [127], G. Simonetti [36], R. Singaraju [130], R. Singh [78], S. Singha [78,130], V. Singhal [130], B.C. Sinha [130], T. Sinha [100], B. Sitar [38], M. Sitta [32], T.B. Skaali [22], K. Skjerdal [18], M. Slupecki [121], N. Smirnov [135], R.J.M. Snellings [56], T.W. Snellman [121], C. Søgaard [34], R. Soltz [74], J. Song [95], M. Song [136], Z. Song [7], F. Soramel [30], S. Sorensen [123], M. Spacek [39], E. Spiriti [71], I. Sputowska [115], M. Spyropoulou-Stassinaki [87], B.K. Srivastava [94], J. Stachel [92], I. Stan [61], G. Stefanek [76], M. Steinpreis [20], E. Stenlund [34], G. Steyn [64], J.H. Stiller [92], D. Stocco [112], P. Strmen [38], A.A.P. Suaide [118], T. Sugitate [46], C. Suire [50], M. Suleymanov [16], R. Sultanov [57], M. Šumbera [82], T.J.M. Symons [73], A. Szabo [38], A. Szanto de Toledo [118,i], I. Szarka [38], A. Szczepankiewicz [36], M. Szymanski [132], J. Takahashi [119], N. Tanaka [126], M.A. Tangaro [33], J.D. Tapia Takaki [50,ii], A. Tarantola Peloni [52], M. Tariq [19], M.G. Tarzila [77], A. Tauro [36], G. Tejeda Muñoz [2], A. Telesca [36], K. Terasaki [125], C. Terrevoli [30,25], B. Teyssier [128], J. Thäder [96,73], D. Thomas [116], R. Tieulent [128], A.R. Timmins [120], A. Toia [52], S. Trogolo [110], V. Trubnikov [3], W.H. Trzaska [121], T. Tsuji [125], A. Tumkin [98], R. Turrisi [107], T.S. Tveter [22], K. Ullaland [18], A. Uras [128], G.L. Usai [25], A. Utrobicic [127], M. Vajzer [82], M. Vala [58], L. Valencia Palomo [69], S. Vallero [27], J. Van Der Maarel [56], J.W. Van Hoorne [36], M. van Leeuwen [56], T. Vanat [82], P. Vande Vyvre [36], D. Varga [134], A. Vargas [2], M. Vargyas [121], R. Varma [47], M. Vasileiou [87], A. Vasiliev [99], A. Vauthier [70], V. Vechernin [129], A.M. Veen [56], M. Veldhoen [56], A. Velure [18], M. Venaruzzo [72], E. Vercellin [27], S. Vergara Limón [2], R. Vernet [8], M. Verweij [133], L. Vickovic [114], G. Viesti [30,i], J. Viinikainen [121], Z. Vilakazi [124], O. Villalobos Baillie [101], A. Vinogradov [99], L. Vinogradov [129], Y. Vinogradov [98], T. Virgili [31], V. Vislavicius [34], Y.P. Viyogi [130], A. Vodopyanov [65], M.A. Völkl [92], K. Voloshin [57], S.A. Voloshin [133], G. Volpe [36,134], B. von Haller [36], I. Vorobyev [91], D. Vranic [96,36], J. Vrláková [40], B. Vulpescu [69], A. Vyushin [98], B. Wagner [18], J. Wagner [96], H. Wang [56], M. Wang [7,112], Y. Wang [92], D. Watanabe [126], M. Weber [36], S.G. Weber [96], J.P. Wessels [53], U. Westerhoff [53], J. Wiechula [35], J. Wikne [22], M. Wilde [53], G. Wilk [76], J. Wilkinson [92], M.C.S. Williams [104], B. Windelband [92], M. Winn [92], C.G. Yaldo [133], Y. Yamaguchi [125], H. Yang [56], P. Yang [7], S. Yano [46], Z. Yin [7], H. Yokoyama [126], I.-K. Yoo [95], V. Yurchenko [3], I. Yushmanov [99], A. Zaborowska [132], V. Zaccolo [79], A. Zaman [16], C. Zampolli [104], H.J.C. Zanoli [118], S. Zaporozhets [65], A. Zarochentsev [129], P. Závada [59], N. Zaviyalov [98], H. Zbroszczyk [132], I.S. Zgura [61], M. Zhalov [84], H. Zhang [18,7], X. Zhang [73], Y. Zhang [7], C. Zhao [22], N. Zhigareva [57], D. Zhou [7], Y. Zhou [79,56], Z. Zhou [18], H. Zhu [18,7], J. Zhu [112,7], X. Zhu [7], A. Zichichi [12,28], A. Zimmermann [92], M.B. Zimmermann [53,36], G. Zinovjev [3], M. Zyzak [42]

[1] *A.I. Alikhanyan National Science Laboratory (Yerevan Physics Institute) Foundation, Yerevan, Armenia*
[2] *Benemérita Universidad Autónoma de Puebla, Puebla, Mexico*
[3] *Bogolyubov Institute for Theoretical Physics, Kiev, Ukraine*
[4] *Bose Institute, Department of Physics and Centre for Astroparticle Physics and Space Science (CAPSS), Kolkata, India*
[5] *Budker Institute for Nuclear Physics, Novosibirsk, Russia*
[6] *California Polytechnic State University, San Luis Obispo, CA, United States*
[7] *Central China Normal University, Wuhan, China*
[8] *Centre de Calcul de l'IN2P3, Villeurbanne, France*
[9] *Centro de Aplicaciones Tecnológicas y Desarrollo Nuclear (CEADEN), Havana, Cuba*
[10] *Centro de Investigaciones Energéticas Medioambientales y Tecnológicas (CIEMAT), Madrid, Spain*
[11] *Centro de Investigación y de Estudios Avanzados (CINVESTAV), Mexico City and Mérida, Mexico*
[12] *Centro Fermi – Museo Storico della Fisica e Centro Studi e Ricerche "Enrico Fermi", Rome, Italy*
[13] *Chicago State University, Chicago, IL, United States*
[14] *China Institute of Atomic Energy, Beijing, China*
[15] *Commissariat à l'Energie Atomique, IRFU, Saclay, France*

[16] COMSATS Institute of Information Technology (CIIT), Islamabad, Pakistan
[17] Departamento de Física de Partículas and IGFAE, Universidad de Santiago de Compostela, Santiago de Compostela, Spain
[18] Department of Physics and Technology, University of Bergen, Bergen, Norway
[19] Department of Physics, Aligarh Muslim University, Aligarh, India
[20] Department of Physics, Ohio State University, Columbus, OH, United States
[21] Department of Physics, Sejong University, Seoul, South Korea
[22] Department of Physics, University of Oslo, Oslo, Norway
[23] Dipartimento di Elettrotecnica ed Elettronica del Politecnico, Bari, Italy
[24] Dipartimento di Fisica dell'Università 'La Sapienza' and Sezione INFN, Rome, Italy
[25] Dipartimento di Fisica dell'Università and Sezione INFN, Cagliari, Italy
[26] Dipartimento di Fisica dell'Università and Sezione INFN, Trieste, Italy
[27] Dipartimento di Fisica dell'Università and Sezione INFN, Turin, Italy
[28] Dipartimento di Fisica e Astronomia dell'Università and Sezione INFN, Bologna, Italy
[29] Dipartimento di Fisica e Astronomia dell'Università and Sezione INFN, Catania, Italy
[30] Dipartimento di Fisica e Astronomia dell'Università and Sezione INFN, Padova, Italy
[31] Dipartimento di Fisica 'E.R. Caianiello' dell'Università and Gruppo Collegato INFN, Salerno, Italy
[32] Dipartimento di Scienze e Innovazione Tecnologica dell'Università del Piemonte Orientale and Gruppo Collegato INFN, Alessandria, Italy
[33] Dipartimento Interateneo di Fisica 'M. Merlin' and Sezione INFN, Bari, Italy
[34] Division of Experimental High Energy Physics, University of Lund, Lund, Sweden
[35] Eberhard Karls Universität Tübingen, Tübingen, Germany
[36] European Organization for Nuclear Research (CERN), Geneva, Switzerland
[37] Faculty of Engineering, Bergen University College, Bergen, Norway
[38] Faculty of Mathematics, Physics and Informatics, Comenius University, Bratislava, Slovakia
[39] Faculty of Nuclear Sciences and Physical Engineering, Czech Technical University in Prague, Prague, Czech Republic
[40] Faculty of Science, P.J. Šafárik University, Košice, Slovakia
[41] Faculty of Technology, Buskerud and Vestfold University College, Vestfold, Norway
[42] Frankfurt Institute for Advanced Studies, Johann Wolfgang Goethe-Universität Frankfurt, Frankfurt, Germany
[43] Gangneung-Wonju National University, Gangneung, South Korea
[44] Gauhati University, Department of Physics, Guwahati, India
[45] Helsinki Institute of Physics (HIP), Helsinki, Finland
[46] Hiroshima University, Hiroshima, Japan
[47] Indian Institute of Technology Bombay (IIT), Mumbai, India
[48] Indian Institute of Technology Indore, Indore (IITI), India
[49] Inha University, Incheon, South Korea
[50] Institut de Physique Nucléaire d'Orsay (IPNO), Université Paris-Sud, CNRS-IN2P3, Orsay, France
[51] Institut für Informatik, Johann Wolfgang Goethe-Universität Frankfurt, Frankfurt, Germany
[52] Institut für Kernphysik, Johann Wolfgang Goethe-Universität Frankfurt, Frankfurt, Germany
[53] Institut für Kernphysik, Westfälische Wilhelms-Universität Münster, Münster, Germany
[54] Institut Pluridisciplinaire Hubert Curien (IPHC), Université de Strasbourg, CNRS-IN2P3, Strasbourg, France
[55] Institute for Nuclear Research, Academy of Sciences, Moscow, Russia
[56] Institute for Subatomic Physics of Utrecht University, Utrecht, Netherlands
[57] Institute for Theoretical and Experimental Physics, Moscow, Russia
[58] Institute of Experimental Physics, Slovak Academy of Sciences, Košice, Slovakia
[59] Institute of Physics, Academy of Sciences of the Czech Republic, Prague, Czech Republic
[60] Institute of Physics, Bhubaneswar, India
[61] Institute of Space Science (ISS), Bucharest, Romania
[62] Instituto de Ciencias Nucleares, Universidad Nacional Autónoma de México, Mexico City, Mexico
[63] Instituto de Física, Universidad Nacional Autónoma de México, Mexico City, Mexico
[64] iThemba LABS, National Research Foundation, Somerset West, South Africa
[65] Joint Institute for Nuclear Research (JINR), Dubna, Russia
[66] Konkuk University, Seoul, South Korea
[67] Korea Institute of Science and Technology Information, Daejeon, South Korea
[68] KTO Karatay University, Konya, Turkey
[69] Laboratoire de Physique Corpusculaire (LPC), Clermont Université, Université Blaise Pascal, CNRS-IN2P3, Clermont-Ferrand, France
[70] Laboratoire de Physique Subatomique et de Cosmologie, Université Grenoble-Alpes, CNRS-IN2P3, Grenoble, France
[71] Laboratori Nazionali di Frascati, INFN, Frascati, Italy
[72] Laboratori Nazionali di Legnaro, INFN, Legnaro, Italy
[73] Lawrence Berkeley National Laboratory, Berkeley, CA, United States
[74] Lawrence Livermore National Laboratory, Livermore, CA, United States
[75] Moscow Engineering Physics Institute, Moscow, Russia
[76] National Centre for Nuclear Studies, Warsaw, Poland
[77] National Institute for Physics and Nuclear Engineering, Bucharest, Romania
[78] National Institute of Science Education and Research, Bhubaneswar, India
[79] Niels Bohr Institute, University of Copenhagen, Copenhagen, Denmark
[80] Nikhef, National Institute for Subatomic Physics, Amsterdam, Netherlands
[81] Nuclear Physics Group, STFC Daresbury Laboratory, Daresbury, United Kingdom
[82] Nuclear Physics Institute, Academy of Sciences of the Czech Republic, Řež u Prahy, Czech Republic
[83] Oak Ridge National Laboratory, Oak Ridge, TN, United States
[84] Petersburg Nuclear Physics Institute, Gatchina, Russia
[85] Physics Department, Creighton University, Omaha, NE, United States
[86] Physics Department, Panjab University, Chandigarh, India
[87] Physics Department, University of Athens, Athens, Greece
[88] Physics Department, University of Cape Town, Cape Town, South Africa
[89] Physics Department, University of Jammu, Jammu, India
[90] Physics Department, University of Rajasthan, Jaipur, India
[91] Physik Department, Technische Universität München, Munich, Germany
[92] Physikalisches Institut, Ruprecht-Karls-Universität Heidelberg, Heidelberg, Germany
[93] Politecnico di Torino, Turin, Italy
[94] Purdue University, West Lafayette, IN, United States

[95] Pusan National University, Pusan, South Korea
[96] Research Division and ExtreMe Matter Institute EMMI, GSI Helmholtzzentrum für Schwerionenforschung, Darmstadt, Germany
[97] Rudjer Bošković Institute, Zagreb, Croatia
[98] Russian Federal Nuclear Center (VNIIEF), Sarov, Russia
[99] Russian Research Centre Kurchatov Institute, Moscow, Russia
[100] Saha Institute of Nuclear Physics, Kolkata, India
[101] School of Physics and Astronomy, University of Birmingham, Birmingham, United Kingdom
[102] Sección Física, Departamento de Ciencias, Pontificia Universidad Católica del Perú, Lima, Peru
[103] Sezione INFN, Bari, Italy
[104] Sezione INFN, Bologna, Italy
[105] Sezione INFN, Cagliari, Italy
[106] Sezione INFN, Catania, Italy
[107] Sezione INFN, Padova, Italy
[108] Sezione INFN, Rome, Italy
[109] Sezione INFN, Trieste, Italy
[110] Sezione INFN, Turin, Italy
[111] SSC IHEP of NRC Kurchatov institute, Protvino, Russia
[112] SUBATECH, Ecole des Mines de Nantes, Université de Nantes, CNRS-IN2P3, Nantes, France
[113] Suranaree University of Technology, Nakhon Ratchasima, Thailand
[114] Technical University of Split FESB, Split, Croatia
[115] The Henryk Niewodniczanski Institute of Nuclear Physics, Polish Academy of Sciences, Cracow, Poland
[116] The University of Texas at Austin, Physics Department, Austin, TX, United States
[117] Universidad Autónoma de Sinaloa, Culiacán, Mexico
[118] Universidade de São Paulo (USP), São Paulo, Brazil
[119] Universidade Estadual de Campinas (UNICAMP), Campinas, Brazil
[120] University of Houston, Houston, TX, United States
[121] University of Jyväskylä, Jyväskylä, Finland
[122] University of Liverpool, Liverpool, United Kingdom
[123] University of Tennessee, Knoxville, TN, United States
[124] University of the Witwatersrand, Johannesburg, South Africa
[125] University of Tokyo, Tokyo, Japan
[126] University of Tsukuba, Tsukuba, Japan
[127] University of Zagreb, Zagreb, Croatia
[128] Université de Lyon, Université Lyon 1, CNRS/IN2P3, IPN-Lyon, Villeurbanne, France
[129] V. Fock Institute for Physics, St. Petersburg State University, St. Petersburg, Russia
[130] Variable Energy Cyclotron Centre, Kolkata, India
[131] Vinča Institute of Nuclear Sciences, Belgrade, Serbia
[132] Warsaw University of Technology, Warsaw, Poland
[133] Wayne State University, Detroit, MI, United States
[134] Wigner Research Centre for Physics, Hungarian Academy of Sciences, Budapest, Hungary
[135] Yale University, New Haven, CT, United States
[136] Yonsei University, Seoul, South Korea
[137] Zentrum für Technologietransfer und Telekommunikation (ZTT), Fachhochschule Worms, Worms, Germany

[i] Deceased.
[ii] Also at: University of Kansas, Lawrence, Kansas, United States.